J|A|C|S
COMMUNICATIONS

Published on Web 05/31/2008

Broadly Hysteretic H_2 Adsorption in the Microporous Metal−Organic Framework Co(1,4-benzenedipyrazolate)

Hye Jin Choi, Mircea Dincă, and Jeffrey R. Long*

Department of Chemistry, University of California, Berkeley, California 94720

Received April 2, 2008; E-mail: jrlong@berkeley.edu

Metal−organic frameworks exhibiting high internal surface areas are currently under intense investigation for the storage of hydrogen and other gases.[1] Among these, flexible metal−organic frameworks have attracted considerable attention owing to their unusual stepwise and sometimes hysteretic guest adsorption behavior.[2] Although rarely observed in microporous solids, hysteretic H_2 adsorption is of great interest because it could provide a kinetics-based trapping mechanism for storing hydrogen at modest pressures.[1d,3] To date, however, such behavior has been observed only over narrow pressure ranges, and mainly for materials with a relatively low H_2 storage capacity. Recognizing the promise of certain tetrazolate-bridged frameworks for high-capacity H_2 adsorption,[1f,g] we recently turned our attention to generating related frameworks of greater stability through use of pyrazolate-based bridging ligands. Herein, we show that 1,4-benzenedi(4′-pyrazolyl) (H_2BDP) reacts with a Co^{2+} salt to form a flexible metal−organic framework exhibiting high surface area, unprecedented multiple-step N_2 adsorption, and significant H_2 uptake with wide hysteresis. In addition, a pore-opening/pore-closing mechanism is proposed to explain the hysteretic H_2 adsorption, and the thermodynamics and kinetics of this process are probed.

Reaction of $Co(CF_3SO_3)_2$ with H_2BDP in *N*,*N*-diethylformamide (DEF) at 130 °C afforded purple needle-shaped crystals of Co(BDP)·2DEF·H_2O (**1**). X-ray analysis of a single crystal revealed a tetragonal structure, featuring one-dimensional chains of Co^{2+} ions, each tetrahedrally coordinated by N atoms from four independent BDP^{2-} ligands (see Figure 1). Pairs of Co^{2+} ions along the chains are bridged by two pyrazolate rings, forming a motif that has been observed previously in molecules such as $[Co(dmpz)(Hdmpz)_2]_2$ (Hdmpz = 3,5-dimethylpyrazole).[4] The structure of **1** displays 10 × 10 Å^2 square channels running along the *c* axis of the crystal, which are interconnected through much narrower slit-like openings. The estimated[5] solvent-accessible volume of 0.91 cm^3/g within the channels is occupied by DEF and water molecules.

Compound **1** is readily desolvated to form Co(BDP) (**1d**). A thermogravimetric analysis of **1** indicated a weight loss of 42% upon heating to 135 °C, corresponding to the release of two DEF molecules and one H_2O molecule per formula unit, and no further weight loss up to 420 °C. This result suggests that the high basicity of pyrazolate relative to tetrazolate imparts increased strength to the metal−nitrogen bonds, which in turn confers higher thermal stability to the framework.[1f,6] Upon fully desolvating the material by heating at 170 °C under dynamic vacuum for two days, the X-ray powder diffraction pattern indicated a complete and substantial change of structure. Although the structure of **1d** could not be determined owing to the poor quality of the diffraction data, subsequent exposure to DEF regenerated the structure of **1**. These observations are at least consistent with an accordion-type flexing behavior that closes and opens the channel pores, as previously demonstrated for analogous 1,4-benzenedicarboxylate-bridged frameworks.[2c]

To probe the porosity of **1d**, N_2 gas sorption isotherms were measured at 77 and 87 K (see Figure 2). Remarkably, at 77 K, five

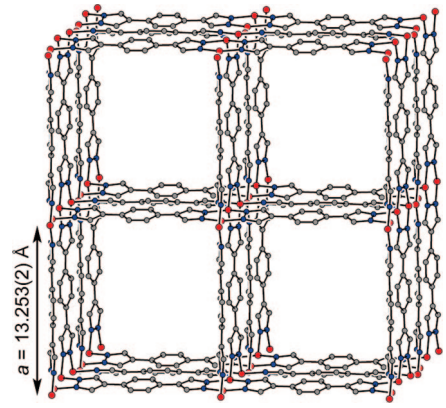

Figure 1. Structure of a portion of the metal−organic framework in **1**, as viewed down the one-dimensional channels running along [001]. Red, gray, and blue spheres represent Co, C, and N atoms, respectively; H atoms are omitted for clarity. Selected interatomic distances (Å) and angles (deg): Co−N, 1.976(5); N−N, 1.378(10); C−N, 1.321(7); Co···Co, 3.543(2); N−Co−N, 109.8(2); Co−N−N, 121.51(3); Co−N−C, 124.7(3).

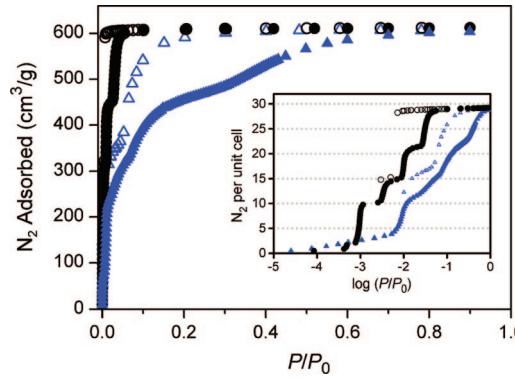

Figure 2. Nitrogen sorption isotherms for **1d** at 77 (black) and 87 (blue) K and pressures of up to 1 bar. Filled and open symbols represent adsorption and desorption data, respectively.

distinct adsorption steps are apparent in the low pressure region of $P/P_0 < 0.05$. At 87 K, the five steps are shifted to higher pressures and are somewhat less distinct, but occur at approximately the same quantities of N_2 adsorbed. Additionally, the desorption of N_2 revealed hysteresis at both temperatures, but was completely reversible at reduced pressure, suggesting that gas sorption involves a pressure-dependent pore-opening/pore-closing process. Note that these sorption isotherms do not conform to any of the IUPAC isotherm types.[7] To our knowledge, an isotherm with as many as five well-resolved steps has never previously been observed for adsorption of a nonpolar gas in any type of microporous material, and the previous record within a metal−organic framework is just two steps, as observed for many flexible framework structures.[2] Such stepwise behavior has generally been attributed to multilayer adsorption on energetically homogeneous

10.1021/ja8024092 CCC: $40.75

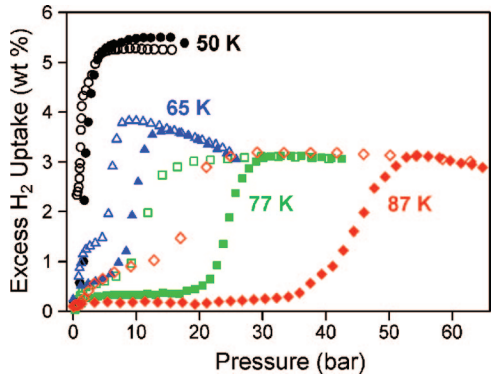

Figure 3. Isotherms for the excess uptake of H_2 within **1d**, showing temperature-dependent hysteresis loops at 50, 65, 77, and 87 K. Filled and open symbols represent adsorption and desorption curves, respectively.

surfaces, multiple adsorbent−adsorbate interactions that substantially differ in energy,[8] or various structural phase transitions occurring under different adsorbate pressures.[2b,c] For **1d**, it is likely that the last of these mechanisms is operational, possibly in conjunction with either or both of the other effects. A Langmuir fit to the N_2 adsorption data for **1d** gave a surface area of 2670 m^2/g, the highest value yet reported for a flexible metal−organic framework. The corresponding pore volume of 0.93 cm^3/g is in good agreement with the solvent accessible volume estimated from the crystal structure of **1**.

Compound **1d** adsorbs almost no H_2 at 77 K and pressures of up to 1.2 bar. This suggests that the pore-opening mechanism is not only temperature- and pressure-dependent, but also gas-dependent, such that the enthalpy and/or entropy changes associated with the adsorption of a given gas play significant roles in the pore opening process. Indeed, as shown in Figure 3, when the pressure is increased, after a low initial plateau, the H_2 uptake abruptly rises at ca. 20 bar and quickly reaches an excess capacity of 3.1 wt % at 30 bar. Importantly, desorption of H_2 only begins at ca.15 bar, resulting in a hysteresis loop with a width of 13 bar. Such a broad, well-defined H_2 sorption hysteresis loop has never previously been reported for a metal−organic framework, and the behavior is reminiscent of metal alloys wherein metal hydride formation leads to large differences in the adsorption and desorption pressures.[9] Similar hysteresis loops have, however, been observed with the adsorption of CO_2, O_2, H_2O, MeOH, or EtOH in other flexible metal−organic frameworks,[2] wherein phase transitions are typically attributed to significant adsorbent−adsorbate or adsorbate−adsorbate interactions via hydrogen-bonding or dipole−dipole contacts. However, since H_2 is nonpolar, such interactions are unlikely to contribute to the observed hysteresis. Instead, the hysteretic behavior in **1d** must be governed by phase transitions with considerably smaller energy barriers, comparable in magnitude to the H_2 adsorption enthalpy.

Intriguingly, hysteretic adsorption could potentially lead to an effective means of H_2 storage, since a large hysteresis loop allows the gas to be stored at lower, safer pressures, while a high charging pressure contributes to an increase in the amount of usable H_2. To probe the influence of temperature on the gating pressure and hysteresis width, H_2 sorption isotherms were measured for **1d** between 50 and 87 K (see Figure 3). Hysteresis is apparent at all temperatures, with the width of the loop increasing from 1.1 to 3.8, 13, and 27 bar upon going from 50 to 65, 77, and 87 K, respectively. In addition, the adsorption branch of each loop shifts toward higher pressure with increasing temperature. Such behavior has been observed previously with other gases, as for example with the adsorption of CH_4 in Cu(4,4′-bipyridine)$_2$(BF_4)$_2$,[10] and has been explained as relating to the rate at which the gas molecules strike the solid surface under supercritical conditions. This rate is proportional to $PT^{-1/2}$, thus causing both

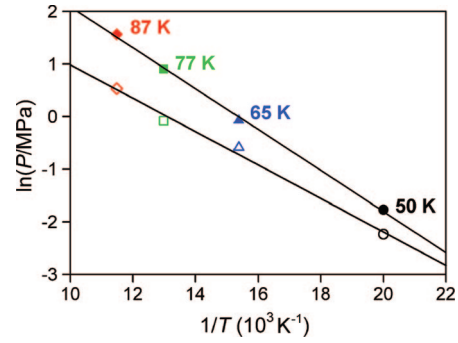

Figure 4. Extrapolation fits for the pore opening (filled symbols) and pore closing (open symbols) pressures in **1d** as a function of temperature.

adsorption and desorption curves to shift to higher pressure with increasing temperature.[11]

Compound **1d** also exhibits a temperature dependence of the excess H_2 uptake capacity. While the solid adsorbs an excess of 5.5 wt % H_2 at 10 bar and 50 K, the maximum uptake decreases to 3.6 and 3.1 wt. % at 65 and 77 K, respectively. This effect is a result of an equilibrium shift between the concentrations of the adsorbed species and the gas phase molecules: a lower thermal energy reduces the evaporation rate and shifts the equilibrium toward the adsorbed species. Although rarely reported, measurements of H_2 uptake below 77 K can provide important information because they allow estimation of the saturation gas storage capacity of a given material.[1j] With a capacity of at least 5.5 wt %, the H_2 loading within **1d** is still significantly below the highest storage capacities reported for metal−organic frameworks.[1e,i,j] Note that the result at 50 K suggests that at 77 or 87 K, additional hysteretic adsorption steps may become apparent at still higher H_2 pressures (as observed for N_2 adsorption).

Given that the hysteresis loops in the H_2 isotherms for **1d** are likely the result of structural phase transitions stimulated by gas adsorption, the thermodynamics of the two concomitant processes cannot be deconvoluted using routine experiments. However, the temperature dependence of the hysteresis width can be used to estimate the overall thermodynamics of the system. Thus, by assuming that **1d** encapsulates H_2 to form a clathrate complex, **1d:H_2**, and by estimating the formation enthalpy of the clathrate, ΔH_f, using the Clausius−Clapeyron equation,

$$\mathrm{d}(\ln P)/\mathrm{d}(1/T) = \Delta H_f/zR \qquad (1)$$

where z is the compression factor, and R is the real gas constant; the pore-opening pressure can be approximated as the vapor pressure of the clathrate complex.[12] The derivative functions of the adsorption and desorption branches of each hysteresis loop were calculated, and the maxima were taken as the respective pore-opening and pore-closing pressures. As shown in Figure 4, plots of ln P versus $1/T$ are linear for both adsorption and desorption data. The slopes of the linear fits, which are equated to $\Delta H_f/R$, give values of 3.2 and 2.6 kJ/mol for the formation and dissociation enthalpies of **1d:H_2**, respectively. This suggests that part of the heat of H_2 adsorption, typically 5 to 11 kJ/mol for metal−organic frameworks,[1h] is consumed during the gate-opening process. Consequently, the formation enthalpy of 3.2 kJ/mol, can be used to estimate that the enthalpy of the pore-opening process for **1d** ought to lie in the range 2−8 kJ/mol.

Notably, extrapolation of the two lines in Figure 4 reveals an intersection point at T = 39 K, where the H_2 adsorption isotherm is expected to show complete reversibility with no hysteresis. Although less reliable, extrapolation in the opposite direction suggests that adsorption of H_2 at 298 K should exhibit a very large hysteresis, with adsorption/pore-opening and desorption/pore-closing occurring at 1100 and 220 bar, respectively.

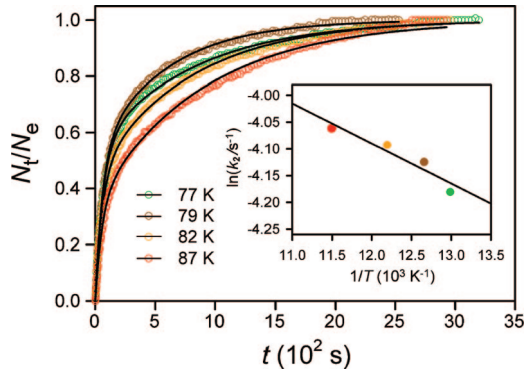

Figure 5. Kinetics profiles for the adsorption of H_2 within **1d** at temperatures between 77 and 87 K. Solid lines represent fits to the data using eq 2. The inset shows the Arrhenius plot corresponding to the diffusion of H_2 along the pore cavities.

To investigate the mechanism of the gated adsorption of H_2 within **1d**, kinetics profiles were measured over a narrow temperature range where the compound was expected to display comparable uptake capacities (77−87 K). In these experiments, samples were exposed to a pressure of H_2 in the range of 67−77 bar, and the amount of H_2 adsorbed was monitored as a function of time. As shown in Figure 5, the kinetics profiles at 77, 79, 82, and 87 K exhibit exponential behavior and could be fit using a double-exponential expression employed previously to model gas sorption kinetics in metal−organic frameworks:[13]

$$N_t/N_e = A_1(1 - e^{-k_1 t}) + A_2(1 - e^{-k_2 t}) \quad (2)$$

where N_t and N_e represent the adsorbed amount of H_2 at time t and at equilibrium, respectively, k_1 and k_2 are the rate constants, and A_1 and A_2 are the relative contributions of two distinct barriers controlling the overall adsorption, with $A_1 + A_2 = 1$. This model assumes the existence of two barriers associated with (i) diffusion at the pore entrance, which is also influenced by the pore-opening process, and (ii) diffusion along the pore cavities.

Fitting each kinetics profile using the foregoing model, while allowing a free refinement of A_1 and A_2, gave rise to a sequence of values for the two rate constants, one of which was larger for all temperatures (see Table S7 in the Supporting Information). The consistently larger value was assigned to k_2, corresponding to the diffusion of H_2 within the pore cavities, which is indeed expected to be very fast. The smaller value, k_1, is associated with the rate-determining step of the adsorption profile, which is thus the overall process associated with the opening of the pores. As mentioned before, this process is likely composed of multiple steps, including a structural phase transition, the pore opening, and gas diffusion through the pore entrance; k_1 is therefore best expressed as $k_{obs(1)}$, representing a combination of steps. Indeed, attempts to obtain a linear fit from an Arrhenius plot employing k_1 values were unsuccessful, confirming a complex mechanism that requires a more advanced kinetic model.

Notably, a linear fit to an Arrhenius plot of ln(k_2) versus 1/T enabled estimation of a barrier of 0.62 kJ/mol for the diffusion of H_2 along the pore cavities of **1d** (see Figure 5, inset). The result is in reasonable agreement with values obtained for the diffusion of H_2 within zeolites, where activation barriers of 1−3 kJ/mol were determined by Monte Carlo molecular dynamics simulations and confirmed using quasi-elastic neutron scattering.[14] To our knowledge, this represents the first assessment of an H_2 diffusion barrier within a metal−organic framework.

The foregoing results demonstrate the utility of BDP^{2-} in generating a flexible metal−organic framework with good thermal stability and a high internal surface area. Most importantly, the compound exhibits high-capacity H_2 adsorption with temperature-dependent hysteresis, enabling assessment of the thermodynamics and kinetics of pore opening/closing processes, and suggesting the potential utility of such compounds for hydrogen storage via a kinetics-based trapping mechanism. Future efforts will focus on assessing the H_2 adsorption properties at higher temperatures and pressures and on enhancing the uptake capacity and H_2 binding affinity within such materials.

Acknowledgment. This research was funded by General Motors Corporation. We thank Dr. A. Dailly and Dr. E. Poirier for experimental assistance and Dr. S. Horike and Dr. F. J. Hollander for helpful discussions.

Supporting Information Available: Complete experimental details; an X-ray crystallographic file (CIF). This material is available free of charge via the Internet at http://pubs.acs.org.

References

(1) (a) Noro, S.; Kitagawa, S.; Kondo, M.; Seki, K. *Angew. Chem., Int. Ed.* **2000**, *39*, 2081. (b) Eddaoudi, M.; Kim, J.; Rosi, N.; Vodak, D.; Wachter, J.; O'Keeffe, M.; Yaghi, O. M. *Science* **2002**, *295*, 469. (c) Rosi, N. L.; Eckert, J.; Eddaoudi, M.; Vodak, D. T.; Kim, J.; O'Keeffe, M.; Yaghi, O. M. *Science* **2003**, *300*, 1127. (d) Férey, G.; Latroche, M.; Serre, C.; Millange, F.; Loiseau, T.; Percheron-Guégan, A. *Chem. Commun.* **2003**, 2976. (e) Wong-Foy, A. G.; Matzger, A. J.; Yaghi, O. M. *J. Am. Chem. Soc.* **2006**, *128*, 3494. (f) Dincă, M.; Yu, A. F.; Long, J. R. *J. Am. Chem. Soc.* **2006**, *128*, 8904. (g) Dincă, M.; Dailly, A.; Liu, Y.; Brown, C. M.; Neumann, D. A.; Long, J. R. *J. Am. Chem. Soc.* **2006**, *128*, 16876. (h) Collins, D. J.; Zhou, H.-C. *J. Mater. Chem.* **2007**, *17*, 3154. (i) Kaye, S. S.; Dailly, A.; Yaghi, O. M.; Long, J. R. *J. Am. Chem. Soc.* **2007**, *129*, 4176. (j) Zhou, W.; Wu, H.; Hartman, M. R.; Yildirim, T. *J. Phys. Chem. C* **2007**, *111*, 16131. (k) Férey, G. *Chem. Soc. Rev.* **2008**, *37*, 191.

(2) (a) Cussen, E. J.; Claridge, J. B.; Rosseinsky, M. J.; Kepert, C. J. *J. Am. Chem. Soc.* **2002**, *124*, 9574. (b) Maji, T. K.; Mostafa, G.; Matsuda, R.; Kitagawa, S. *J. Am. Chem. Soc.* **2005**, *127*, 17152. (c) Llewellyn, P. L.; Bourrelly, S.; Serre, C.; Filinchuk, Y.; Férey, G. *Angew. Chem., Int. Ed.* **2006**, *45*, 7751. (d) Kondo, A.; Noguchi, H.; Carlucci, L.; Proserpio, D. M.; Ciani, G.; Kajiro, H.; Ohba, T.; Kanoh, H.; Kaneko, K. *J. Am. Chem. Soc.* **2007**, *129*, 12362. (e) Serre, C.; Mellot-Draznieks, C.; Surblé, S.; Audebrand, N.; Filinchuk, Y.; Férey, G. *Science* **2007**, *315*, 1828.

(3) (a) Zhao, X.; Xiao, B.; Fletcher, A. J.; Thomas, K. M.; Bradshaw, D.; Rosseinsky, M. J. *Science* **2004**, *306*, 1012. (b) Yang, C.; Wang, X.; Omary, M. A. *J. Am. Chem. Soc.* **2007**, *129*, 15454.

(4) Ehlert, M. K.; Rettig, S. J.; Storr, A.; Thompson, R. C.; Trotter, J. *Can. J. Chem.* **1993**, *71*, 1425.

(5) Spek, A. L. *PLATON*; The University of Utrecht: Utrecht, The Netherlands, 1999.

(6) (a) High thermal stability has been recognized recently in several other pyrazolate-bridged frameworks: He, J.; Yin, Y.-G.; Wu, T.; Li, D.; Huang, X.-C. *Chem. Commun.* **2006**, 2845. (b) Zhang, J.-P.; Kitagawa, S. *J. Am. Chem. Soc.* **2008**, *130*, 907. (c) Tekarli, S. M.; Cundari, T. R.; Omary, M. A. *J. Am. Chem. Soc.* **2008**, *130*, 1669.

(7) Sing, K. S. W.; Everett, D. H.; Haul, R. A. W.; Moscou, L.; Pierotti, R. A.; Rouquerol, J.; Siemieniewska, T. *Pure Appl. Chem.* **1985**, *57*, 603.

(8) (a) Gregg, S. J.; Sing, K. S. W. *Adsorption, Surface Area and Prorosity*; Academic Press, 2nd ed. 1982, pp. 1−18, and 84–89. (b) Walton, K. S.; Millward, A. R.; Dubbeldam, D.; Frost, H.; Low, J. J.; Yaghi, O. M.; Snurr, R. Q. *J. Am. Chem. Soc.* **2008**, *130*, 406.

(9) Wang, D.; Noh, H.; Flanagan, T. B.; Balasubramaniam, R. *J. Alloys Comp.* **2003**, *348*, 199.

(10) Noguchi, H.; Kondoh, A.; Hattori, Y.; Kanoh, H.; Kajiro, H.; Kaneko, K. *J. Phys. Chem. B* **2005**, *109*, 13851.

(11) Do, D. D. *Adsorption Analysis: Equilibria and Kinetics*; Imperial College Press: Vol. 2, 1998; pp 1−18.

(12) Waals, J. H.; Platteeuw, J. C. *Adv. Chem. Phys.* **1959**, *2*, 1.

(13) Fletcher, A. J.; Cussen, E. J.; Bradshaw, D.; Rosseinsky, M. J.; Thomas, K. M. *J. Am. Chem. Soc.* **2004**, *126*, 9750.

(14) (a) Jhi, S.-H. *Microporous Mesoporous Mater.* **2006**, *89*, 138. (b) Anil Kumar, A. V.; Jobic, H.; Bhatia, S. K. *Adsorption* **2007**, *13*, 501.

JA8024092